Anion Coordination

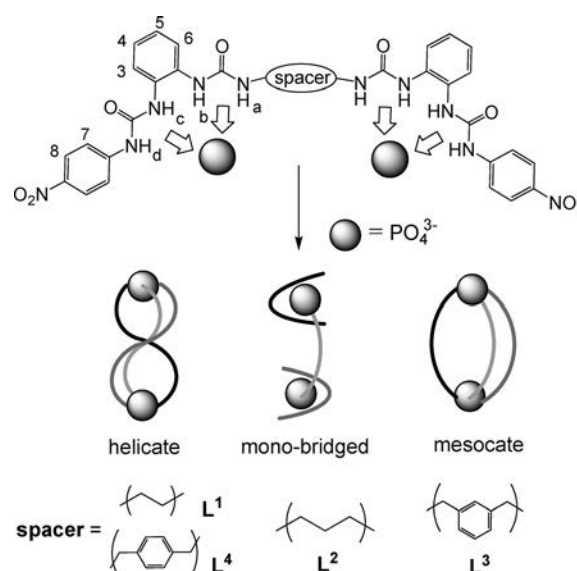# The Effect of the Spacer of Bis(biurea) Ligands on the Structure of A₂L₃-type (A = anion) Phosphate Complexes

Biao Wu,*[a] Shaoguang Li,[b] Yibo Lei,[a] Huaiming Hu,[a] Nader de Sousa Amadeu,[c] Christoph Janiak,[c] Jennifer S. Mathieson,[d] De-Liang Long,[d] Leroy Cronin,[d] and Xiao-Juan Yang*[a]

Abstract: By tuning the length and rigidity of the spacer of bis(biurea) ligands L, three structural motifs of the A₂L₃ complexes (A represents anion, here orthophosphate PO_4^{3-}), namely helicate, mesocate, and mono-bridged motif, have been assembled by coordination of the ligand to phosphate anion. Crystal structure analysis indicated that in the three complexes, each of the phosphate ions is coordinated by twelve hydrogen bonds from six surrounding urea groups. The anion coordination properties in solution have also been studied. The results further demonstrate the coordination behavior of phosphate ion, which shows strong tendency for coordination saturation and geometrical preference, thus allowing for the assembly of novel anion coordination-based structures as in transition-metal complexes.

Introduction

Control of supramolecular self-assembly to yield desired structures and functions is a fundamental goal for chemists, wherein rational design of the ligands (or hosts) and careful choice of the coordination centers (guests) are key factors. Among various metal coordination-based supramolecular systems, helical complexes (helicates) are a very important class of structures because of their significant aesthetic and biomimetic attractions.[1–5] For the M₂L₃ complexes with two octahedral metal ions and three bis(bidentate) ligands, two possible triply bridged structures are normally encountered: the homochiral helicates where the two metal centers display identical absolute configurations (ΔΔ or ΛΛ) and the achiral *meso*-helicates (also called mesocates) in which the metal ions possess opposite configurations (ΔΛ) (Scheme 1).[6] Although far less common, there is also a mono-bridged motif for the M₂L₃-type

[a] Prof. B. Wu, Prof. Y. Lei, Prof. H. Hu, Prof. X.-J. Yang
Key Laboratory of Synthetic and Natural Functional Molecule Chemistry of the Ministry of Education, College of Chemistry and Materials Science
Northwest University, Xi'an 710069 (P. R. China)
E-mail: wubiao@nwu.edu.cn
         yangxiaojuan@nwu.edu.cn

[b] Dr. S. Li
State Key Laboratory for Oxo Synthesis & Selective Oxidation
Lanzhou Institute of Chemical Physics, CAS
Lanzhou 730000 (P. R. China)

[c] Dr. N. de Sousa Amadeu, Prof. Dr. C. Janiak
Institut für Anorganische Chemie und Strukturchemie
Universität Düsseldorf
Universitätsstrasse 1, 40225, Düsseldorf (Germany)

[d] Dr. J. S. Mathieson, Dr. D.-L. Long, Prof. L. Cronin
WestCHEM, School of Chemistry, University of Glasgow
University Avenue, Glasgow G12 8QQ, Scotland (UK)

⬛ Supporting information for this article is available on the WWW under http://dx.doi.org/10.1002/chem.201405234.

Scheme 1. Various structural motifs (helicate, mono-bridged, and mesocate) of the [A₂L₃] anion complexes with bis(biurea) ligands bearing different spacers (L¹–L⁴).

complexes in which only one bis(bidentate) ligand functions as a bridge between the two metal ions while each of the other two ligands chelates a metal ion in the terminal tetradentate fashion (Scheme 1). To control the formation of these structures, thorough investigations have been carried out on the self-assembly processes, in particular the influences of ligands.[7] On the basis of studies on a series of dicatechol ligands with an alkyl spacer, Albrecht[8] suggested the empirical odd–even rule that demonstrates the effect of the alkyl spacer on the structure of M₂L₃ complexes. With an even number of carbon atoms (methylene groups) of the alkyl linker, the ligand

tends to adopt the *S* conformation and a helicate is preferred. In contrast, when the alkyl linker has an odd number of carbon atoms, the ligand will display the *C* conformation, and thus favors a mesocate structure (Scheme 1).

Anion coordination chemistry has been rapidly developed and applied in anion binding in recent years. It has been shown that anions also display some stereoelectronic and geometrical preference as the transition-metal ions.[9, 10] Therefore, it should be possible to construct novel anion-based structures such as cages, knots, and helicates in which the coordination centers are anions instead of metal ions.[11] Although this area is still under exploration, it already led to an exciting branch of coordination chemistry. Inspired by the coordination behavior of the well-known oligo-pyridine ligands, we have recently designed a class of oligo-urea anion receptors[12] with the *ortho*-phenylene bridge[13] between two urea groups, which has proven to be able to provide complementary anion binding sites. The results clearly demonstrated the resemblance of oligo-urea and oligo-pyridine ligands in anion and metal coordination, in which each urea subunit (two NH donors) indeed serves as a coordination vector towards an anion, like a pyridyl group towards a metal ion. By using a bis(biurea) ligand with an ethylene spacer (L^1), the first triple-stranded anion helicate, $[(PO_4)_2(L^1)_3]^{6-}$ (**1**), was successfully obtained upon coordinating to phosphate ions.[12d]

In the helicate **1**, each phosphate center is coordinated by twelve hydrogen bonds (saturated coordination for tetrahedral anions)[10c] from six urea groups in an approximately octahedral coordination geometry (Scheme 1). This coordination saturation and geometrical preference is very similar to transition-metal ions, which not only endows the anion center chirality, but also ensures the formation of the desired triple-stranded structure. Moreover, the formation of **1** follows the odd–even rule just like the metal helicates with the ethylene spacer. These facts encouraged us to further explore the assembly of the A_2L_3 complexes. It was supposed that the mesocate topology for A_2L_3-type complexes should also be obtained by tuning the spacer of the bis(biurea) building blocks. To this end, a series of bis(biurea) ligands (L^2–L^4) with different spacers (R group; see Scheme 1) have been synthesized. Herein we report the self-assembly of dinuclear phosphate complexes with these bis(biurea) ligands both in the solid state and in solution. It is very interesting that three types of structures, including the less common, mono-bridged motif (**2**), the mesocate (**3**), and the helicate (**4**), have been obtained from these ligands (Scheme 1).

Results and Discussion

Synthesis and crystal structures of the phosphate complexes 2–4

From a mixture of L^2, K_3PO_4, and 18-crown-6, crystals of complex **2** with the composition $[K(18\text{-crown-}6)]_6[(PO_4)_2(L^2)_3]\cdot 3\,Et_2O\cdot 2\,Me_2CO\cdot H_2O$ were isolated in high yield (>85%). Surprisingly, although the complex has the anion-to-ligand ratio of 2:3 (A_2L_3), it does not display the triple-stranded mesocate
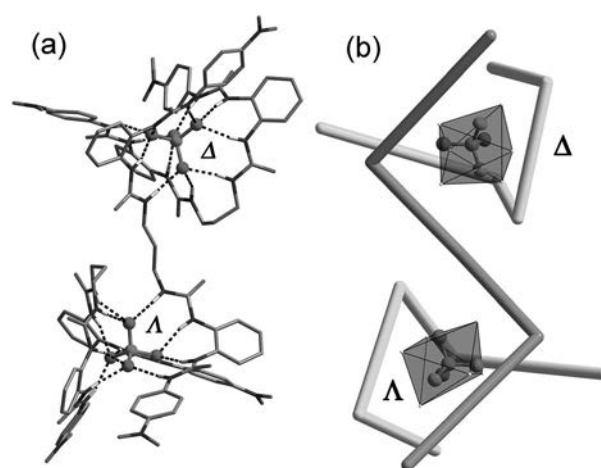

Figure 1. a) Molecular structure of the mono-bridged $[(PO_4)_2(L^2)_3]^{6-}$ (**2**), and b) illustration of the different ligand conformations in this *meso*-structure. The two PO_4^{3-} coordination octahedra were generated by connecting the six coordination vectors (urea groups). Other atoms and groups were omitted for clarity. (A color version of this figure can be found in the Supporting Information).

structure expected for ligand L^2 with an odd spacer (propylene). Instead, the mono-bridged motif (Figure 1 and Scheme 1) was formed, which is an unusual alternative of the triple-stranded architectures. In the $[(PO_4)_2(L^2)_3]^{6-}$ complex, only one of the three ligands acts as a bridge between the two phosphate ions, while the other two ligands function in a terminal "tetradentate" chelating manner to bind the two anions. The bridging ligand adopts a "C"-shaped (AA-*trans*) conformation for the propylene spacer, but its two biurea moieties are arranged in an *anti* fashion. The other two ligands adopt such a conformation that three of the urea groups are roughly coplanar, occupying three edges of a square, while the fourth urea arm is almost perpendicular to the plane, resulting in a folded GG-*cis* conformation. Thus, each PO_4^{3-} center is actually coordinated by a whole and a half ligand rather than three half ligands found in the triple-bridged helicate or mesocate structure. This mono-bridged topology has been reported in M_2L_3 transition-metal complexes; for example, the iron(III) and nickel(II) coordination architectures with alcaligin (AG) and a tetradentate bis(pyrazolyl pyridine) with an *o*-xylylene space, respectively.[14] Notably, the two anions within one $[(PO_4)_2(L^2)_3]^{6-}$ unit in complex **2** display opposite absolute configurations (Δ and Λ), indicating a *meso*-structure (space group $P2_1/c$).

Nevertheless, within each half of the mono-bridged complex, the PO_4^{3-} ion is coordinated by six urea groups from three biurea domains through twelve hydrogen bonds (N···O distances range from 2.746 (5) to 2.928(5) Å, and N–H···O angles from 149 to 177°; Figure 1, Supporting Information, Table S2). This is similar to the helicate **1** and further reveals the strong binding ability of phosphate ion and its requirement for saturated coordination. The average N···O distance in **2** (2.800 Å) is almost identical to that in the helicate **1** (2.802 Å). Furthermore, as in the helicate structure **1**, T-shaped C—H···π interactions (about 3.6 Å) are also observed in

the *meso* complex **2** between the terminal aromatic rings and *o*-phenylene planes.[15]

In complex **2**, it appears that the propylene spacer has considerable flexibility and can assume both the "C"-shaped bis(bidentate) conformation and the folded tetradentate motif. To evaluate the energy preference of the different conformations, DFT calculations were carried out on the A_2L_3 phosphate complexes of **L²** at the B3LYP/6-31G level. All of the three structures (helicate **a**, mesocate **b**, and mono-bridged motif **c**; Supporting Information, Figure S1) have been built and optimized.[16] The total energies revealed that the mono-bridged species **c** (complex **2**) is indeed the most stable structure, whose energy is 59.5 and 95.9 kJ mol⁻¹ lower than the mesocate (**b**) and helicate (**a**), respectively. This is in good agreement with the experimental formation of complex **2**. Overall the homochiral helicate (**a**) has the highest energy, which is consistent with the odd–even rule that an odd spacer prefers the meso structure rather than the helicate. However, even the lower-energy mesocate **b** was not favored in this case and the structure **c** (complex **2**) was chosen as the optimal mode. The reason why the structure **c** but not **b** was formed might be attributed to the repulsive forces of the three intertwined alkyl groups in model (**b**) as well as ligand strains caused by coordination with the PO_4^{3-} ions.

It should be noted that although most M_2L_3 systems follow the odd–even rule, there are also considerable exceptions in the literature. For instance, Dolphin et al. reported the observation of both helicate and mesocate structures formed by the same bis(dipyrromethene) ligand and studied the isomerization of the two conformers.[17] In some other cases, the triple-stranded helicate is in competition with more complicated structures (for example, tetrahedral cage).[14] Thus, other factors (such as the coordination center, solvent, counterions, and templates) should also be considered when applying this empirical rule.

As the propylene-linked ligand **L²** did not form the triple-bridged anion mesocate, which is partially due to its flexibility, we replaced the propylene spacer with *m*-xylylene, which is semi-rigid and also has an odd number of carbon atoms, and synthesized the bis(biurea) ligand **L³** (Scheme 1). Promisingly, in this case the assembly of ligand **L³** and PO_4^{3-} anion afforded the desired triple-bridged mesocate complex **3** with the composition $[K(18\text{-crown-}6)]_6[(PO_4)_2(L^3)_3]\cdot3\,H_2O$. In the $[(PO_4)_2(L^3)_3]^{6-}$ unit three C-shaped ligands coordinate with two PO_4^{3-} anions to form the dinuclear triple-stranded complex. The two phosphate anion centers, which reside in pseudo-octahedral coordination geometries, assume opposite configurations (Δ/Λ) on the two sides of a mirror plane (Figure 2a). As in the analogous helicate **1**, each phosphate ion is also bound by six urea groups from three different bis(biurea) ligands through twelve hydrogen bonds (N···O distances range from 2.606(3) to 2.994(2) Å, and N—H···O angles from 145 to 168°; Figure 2, Supporting Information, Table S3). The average N···O distance (2.819 Å) in the mesocate **3** is slightly longer than that in **2** and the helicate **1**.

The *p*-xylylene-spaced bis(biurea) ligand **L⁴**, which has a spacer that is one carbon longer than **L³** and thus has an
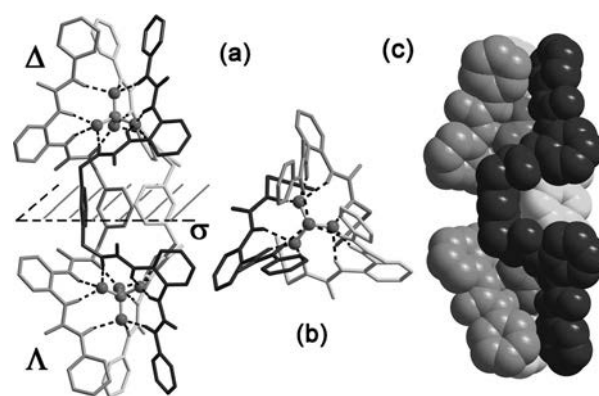

Figure 2. Molecular structure of the mesocate $[(PO_4)_2(L^3)_3]^{6-}$ (**3**). a) Side view, b) top view, and c) space-filling representation. There is a mirror plane (σ) across the *m*-xylylene groups. The counter-cations, non-acidic hydrogen atoms, and nitro groups are omitted for clarity. (A color version of this figure can be found in the Supporting Information).

even number of carbon atoms, gave the expected helicate $[K(18\text{-crown-}6)]_6[(PO_4)_2(L^4)_3]$ (**4**) following the odd–even rule (Scheme 1). In the triple-stranded anion complex $[(PO_4)_2(L^4)_3]^{6-}$, the two phosphate centers assume the same configuration ($\Delta\Delta$ or $\Lambda\Lambda$), each of which is coordinated by six urea groups through twelve hydrogen bonds. Unfortunately, we have only obtained the preliminary crystal structure for this complex, which showed the backbone of the helicate but did not allow further refinement of the structure.

Solution coordination studies of the ligands with phosphate anion

The assembly of the ligands and PO_4^{3-} ions in solution was investigated by UV/Vis, NMR, and ESI-MS techniques. In the case of **L²** (complex **2**), Job's plot of UV/Vis titrations revealed that the ligand and PO_4^{3-} anion form the 3:2 binding mode in DMSO/5 % H_2O (Supporting Information, Figure S2). The ¹H NMR, 2D-TOCSY, 2D-NOE, and 2D-DOSY studies were carried out by using the isolated complex **2** dissolved in [D₆]DMSO. In the ¹H NMR spectrum of **2**, all of the urea NH groups showed very large downfield shifts compared with the free ligand ($\Delta\delta = 3.01$–4.41 ppm; Figure 3a). These values are even larger than those ($\Delta\delta = 2.86$–3.90 ppm) in the helicate **1**, suggesting stronger hydrogen bonding in **2** as also proved by the hydrogen bonding parameters in the crystal structure. An obvious upfield shift ($\Delta\delta = -0.6$ ppm) of the H8 proton on the terminal nitrophenyl rings (see Scheme 1 for the numbering of the protons) was observed that is due to the shielding effects caused by the formation of the anion complex. The most interesting feature of the NMR spectrum, however, is the slow equilibrium of the complex with other components on the NMR timescale (because of the strong interactions between **L²** ligands and PO_4^{3-} ions). This character leads to well-resolved NMR signals and allows for clear elucidation of the structure in solution.

Although the UV/Vis results point to the formation of an $[A_2L_3]$ complex, they are not sufficient for the discrimination among the helicate, mesocate, and mono-bridged motif. To
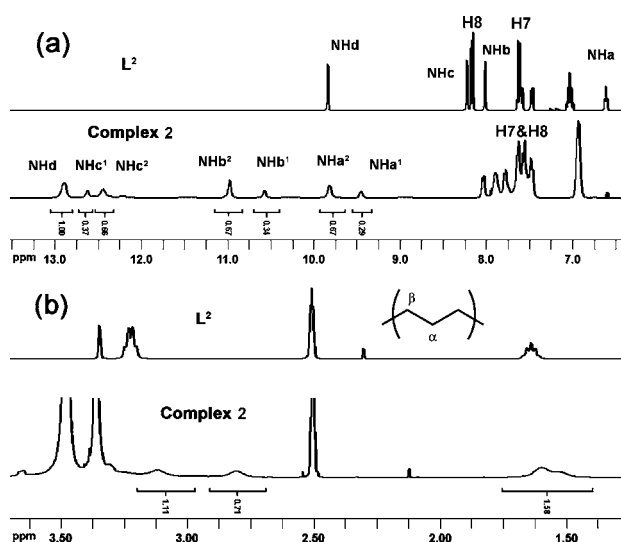
Figure 3. ^{1}H NMR spectra of **L^2** and complex **2** in [D$_6$]DMSO. a) The low- and b) high-field regions (see Scheme 1 for the numbering of the protons).

confirm that the "folded" structure of **2** is preferred in solution, other evidence is necessary. One of the most important features of complex **2** is that the three ligands adopt two conformations, while they are identical in both the C_3-symmetric helicate and mesocate. This difference should be reflected in the NH protons and the CH$_2$CH$_2$CH$_2$ spacer. Notably, the urea NH signals of complex **2** split into two sets with a 2:1 integral ratio, which perfectly demonstrates the presence of two different conformers of the ligands (the tetradentate form and bis-(bidentate) form). Moreover, this splitting decreases when the chemical environment of the NH protons becomes closer, from 152.1 and 176.0 Hz for the "inner" NHa and NHb to complete overlapping (0 Hz) for the far end NHd protons (Figure 3a).

The CH$_2$CH$_2$CH$_2$ spacer is also a good stereochemical probe for determining the topology of the M$_2$L$_3$ complexes.[8a] In the helicate and mesocate, the H$^\beta$ protons (Figure 3b) are diastereotopic, which could result in two multiplets in the ^{1}H NMR spectrum. Moreover, in the helicate, the central H$^\alpha$ protons are enantiotopic, leading to one signal in solution. In contrast, the H$^\alpha$ protons present diastereotopic behavior (two multiplets) in the mesocate. Thus, the propylene protons should show three multiplets in the helicate, but they could exhibit four signals in the mesocate. The situation is even more complicated for the mono-bridged complex **2**. Considering the two different conformations of the three ligands, the H$^\alpha$ protons of the CH$_2$CH$^\alpha_2$CH$_2$ spacer could cause up to three signals (the chemical environments of the two H$^\alpha$ protons in the bridging ligand are very close, but they are different for the terminal ligands) and the H$^\beta$ protons could induce up to four peaks. Therefore, the propylene spacer of **2** might show seven signals (or less if overlap occurs).

Variable-temperature ^{1}H NMR experiments in [D$_6$]DMSO/CDCl$_3$ have been conducted (Supporting Information, Figure S4). At room temperature, two multiplets of the H$^\alpha$ protons and three signals of the H$^\beta$ protons were observed. The total number of visible peaks (five) is less than expected for the

well-resolved spectrum of structure **2** (seven) but is more than three (for helicate) and four (for mesocate), indicating the presence of structure **2**. When the sample was heated, the signals of H$^\alpha$ and H$^\beta$ protons broadened gradually and showed an obvious coalescence at 309 K, indicating the inversion of the configurations at the two coordination centers ($\Delta_1\Lambda_2$ to $\Lambda_1\Delta_2$) on the NMR timescale. This temperature is just slightly higher than room temperature, and the free-energy barrier of the dynamic process was calculated to be 24.1 kJ mol^{-1} (from the Eyring equation).

In the 2D-TOCSY (total correlation spectroscopy) spectrum of complex **2** (Supporting Information, Figures S5, S6), NHa^1 and NHb^1, NHa^2 and NHb^2, NHc^1 and NHd, and NHc^2 and NHd are correlative, which means that they belong to their respective spin systems and further confirms their ^{1}H NMR assignments in Figure 3. The H7 and H8 signals at around 7.6 ppm (7.4–7.7 ppm) can be assigned as a same spin system, and the 2D-NOE spectrum of **2** (Supporting Information, Figure S7) revealed their spatial proximity with the bridging phenylene protons (H3 to H6). The 2D diffusion ordered spectroscopy (2D-DOSY) in [D$_6$]DMSO at 300 K was also performed (Supporting Information, Figure S8). For **L^2**, the measured diffusion coefficient ($D = 1.44 \times 10^{-10}$ m^2 s^{-1}) corresponds to a hydrodynamic radius (r_s, calculated from the Stokes–Einstein equation) of 7.7 Å. For complex **2**, all the peaks correlating to **L^2** are in a horizontal line with a D value of 8.09×10^{-11} m^2 s^{-1}, corresponding to an r_s value of 13.1 Å that is much larger than the single ligand. This radius and the calculated hydrodynamic volume (9412 Å^3) are very close to the estimated rotary radius and volume (13.4 Å, 10051 Å^3) for [(PO$_4$)$_2$(**L^2**)$_3$]$^{6-}$ in the crystal structure of **2** (Supporting Information, Figure S9), which confirmed the persistence of the complex in solution.

ESI-MS studies were carried out for the complexes. In the mono-bridged structure **2**, the A$_2$L$_3$ anion complex [(PO$_4$)$_2$(**L^2**)$_3$] was detected at m/z 1140.8 for [(PO$_4$)$_2$(**L^2**)$_3$H$_2$K$_2$]$^{2-}$ (calcd. 1140.76), 1272.9 for [(PO$_4$)$_2$(**L^2**)$_3$H$_2$K$_2$(18-crown-6)]$^{2-}$ (calcd. 1272.84), and 1405.0 for [(PO$_4$)$_2$(**L^2**)$_3$K$_2$H$_2$(18-crown-6)$_2$]$^{2-}$ (calcd. 1404.92), respectively (Supporting Information, Figure S10 and Table S4). Furthermore, in our previous experiment for the helicate [(PO$_4$)$_2$(**L^1**)$_3$]$^{6-}$ (**1**), the 2:3 species could not be observed. However, by increasing the concentration of the sample, the A$_2$L$_3$ species [(PO$_4$)$_2$(**L^1**)$_3$H$_2$K$_2$(18-crown-6)]$^{2-}$ and [(PO$_4$)$_2$(**L^1**)$_3$H$_2$K$_2$(18-crown-6)]$_2$]$^{2-}$ at m/z 1251.9 and 1383.9 (calcd. 1251.81 and 1383.90), respectively, were observed in CH$_2$Cl$_2$ (Supporting Information, Figure S11 and Table S5). In these MS spectra, however, other fragments, including the deprotonated ligand, and the 1:1, 1:2 and 1:3 (guest to host) anion coordination species, are also present, indicating that the anion complexes are labile during the ionization processes.

Conclusion

A series of new bis(biurea) ligands (with the flexible propylene and semi-rigid m-xylylene and p-xylylene spacer, respectively) coordinate with phosphate ions to generate the A$_2$L$_3$-type anion complexes. The biurea coordination domains exhibited excellent complementarity to the PO$_4$$^{3-}$ ions. Because of the

coordination saturation requirement of the phosphate ion (12 hydrogen bonds) and its octahedral coordination geometry, as well as the intrinsic stereochemical preference of the spacer in the bis(biurea) ligands, these species make ideal building blocks for the construction of novel anion-based architectures similar to those of the metal ion-based systems. By altering the rigidity and conformation of the spacer of bis(biurea) receptors, the three topologies of the A_2L_3 complexes (helicate, mesocate, and mono-bridged structure) can be successfully assembled. The present work provides a helpful approach to the control of the configuration in the self-assembly of helical structures. Furthermore, these results may help the design of new anion ligands and construction of anion-coordination architectures. Assembly of other novel anion coordination-based topologies is currently underway in our laboratory.

Experimental Section

General considerations

o-Nitrophenylisocyanate and p-nitrophenylisocyanate were purchased from Alfa Aesar and used as received. All solvents and other reagents were of reagent-grade quality. ^1H and ^{13}C NMR spectra were recorded on a Mercury plus-400 spectrometer at 400 MHz and 100 MHz, respectively, using TMS as an internal standard. UV/Vis spectra were performed on an HP8453 spectrophotometer (1 cm quartz cell). Elemental analyses were performed on an Elementar VarioEL instrument. IR spectra were recorded on a Bruker IFS 120HR spectrometer. ESI-MS measurements of the ligands and anion complexes were carried out using a Waters ZQ4000 spectrometer and a Bruker MicrOTOF-Q spectrometer, respectively. Melting points were detected on an X-4 Digital Vision MP Instrument.

Synthesis

Detailed synthetic processes for ligands **L²**–**L⁴** are given in the Supporting Information.

L²: Light yellow solid. M.p.: 215 °C. ^1H NMR (400 MHz, [D₆]DMSO, ppm): δ 9.83 (s, 2H, Hd), 8.22 (s, 2H, Hc), 8.17 (d, J=9.2 Hz, 4H, H8), 8.00 (s, 2H, Hb), 7.63 (m, 4H, H7), 7.48 (m, 2H, H3), 7.46 (d, J=8.0 Hz, 2H, H6), 7.03 (m, 4H, H4+H5), 6.61 (s, 2H, Ha), 3.23 (m, 4H, β-CH₂), 1.64 (m, 4H, α-CH₂). ^{13}C NMR (100 MHz, [D₆]DMSO), 156.6 (CO), 152.4 (CO), 146.6 (C), 140.8 (C), 131.6 (C), 125.0 (CH), 124.3 (CH), 123.9 (CH), 106.7 (CH), 36.4 (α-CH₂), 30.1 (β-CH₂). IR (KBr): $\tilde{v}=$ 3357, 3299, 3081, 1664, 1593, 1571, 1500, 1329, 1299 cm^{-1}. Anal. calcd (%) for $C_{31}H_{30}N_{10}O_8$: C 55.52, H 4.51, N 20.89; found: C 55.84, H 4.43, N 20.75. ESI-MS: m/z 100%, 671.2 [M+H]⁺; 40%, 693.2 [M+Na]⁺.

L³: Light yellow solid. M.p.: 274 °C. ^1H NMR (400 MHz, [D₆]DMSO, ppm): δ 9.86 (s, 2H, Hd), 8.25 (s, 2H, Hc), 8.18 (m, 4H, H8), 8.00 (s, 2H, Hb), 7.70 (m, 4H, H7), 7.60 (m, 2H, H3), 7.51 (m, 2H, H6), 7.26 (m, 2H, Hγ), 7.20 (m, 2H, Hα), 7.06 (m, 4H, Hβ), 7.04 (s, 2H, Ha), 4.30 (m, 4H, CH₂). ^{13}C NMR (100 MHz, [D₆]DMSO), 155.9 (CO), 152.7 (CO), 146.7 (C), 140.8 (C), 140.2 (C), 132.8 (C), 129.7 (C), 128.3 (CH), 126.3 (CH), 125.7 (CH), 125.1 (CH), 124.9 (CH, CH), 123.1 (CH), 117.3 (CH), 43.0 (CH₂). IR (KBr): $\tilde{v}=$ 3352, 3299, 3078, 1659, 1593, 1575, 1500, 1327, 1205 cm^{-1}. Anal. calcd (%) for $C_{36}H_{32}N_{10}O_8$: C 59.01, H 4.40, N 19.12; found: C 58.86, H 4.37, N 18.89. ESI-MS: m/z 100%, 733.2 [M+H]⁺; 60%, 755.2 [M+Na]⁺.

L⁴: Light yellow solid. M.p.: >300 °C. ^1H NMR (400 MHz, [D₆]DMSO, ppm): δ 9.87 (s, 2H, Hd), 8.25 (s, 2H, Hc), 8.18 (d, J=8.0 Hz, 4H, H6), 7.99 (s, 2H, Hb), 7.70 (d, J=8.0 Hz, 4H, H5), 7.59 (d, J=8.0 Hz, 2H, H4), 7.51 (d, J=8.0 Hz, 2H, H1), 7.27 (s, 4H, Hα), 7.06 (m, 6H, Ha, H2, H3), 4.28 (d, J=8.0 Hz, 4H, Hβ). ^{13}C NMR (100 MHz, [D₆]DMSO), 155.7 (CO), 152.6 (CO), 146.6 (C), 140.8 (C), 138.6 (C), 132.7 (C), 129.6 (C), 127.2 (CH), 125.1 (CH), 124.9 (CH), 124.7 (CH), 123.2 (CH, CH), 122.9(CH), 117.2 (CH), 42.7 (CH₂). IR (KBr): $\tilde{v}=$ 3354, 3294, 3076, 1655, 1597, 1579, 1502, 1321, 1200 cm^{-1}. Anal. calcd (%) for $C_{36}H_{32}N_{10}O_8$: C 59.01, H 4.40, N 19.12; found: C 58.73, H 4.45, N 18.82. ESI-MS: m/z 100%, 733.2 [M+H]⁺; 70%, 755.2 [M+Na]⁺.

[K(18-crown-6)]₆[(PO₄)₂(**L²**)₃]·3 Et₂O·2 Me₂CO·H₂O (**2**): Ligand **L²** (33.5 mg, 0.5 mmol), K₃PO₄·10 H₂O (18.5 mg, 0.5 mmol), and 18-crown-6 (39.6 mg, 1.5 mmol) were suspended in acetone (5 mL). After stirring for 2 h at room temperature, a clear reddish-orange solution was obtained. Slow vapor diffusion of diethyl ether into this solution provided yellow crystals of complex **2** within 3 days (67 mg, 85%). M.p. 158 °C. Anal. calcd (%) for $C_{165}H_{236}K_6N_{30}O_{69}P_2$: C 49.05, H 5.89, N 10.40; found: C 48.82, H 5.73, N 9.98.

[K(18-crown-6)]₆[(PO₄)₂(**L³**)₃]·3 H₂O (**3**): A mixture of **L³** (36.6 mg, 0.5 mmol), K₃PO₄·10 H₂O (18.5 mg, 0.5 mmol), and 18-crown-6 (39.6 mg, 1.5 mmol) in acetone (5 mL) was stirred for 5 h at room temperature to give an orange solution. Slow vapor diffusion of diethyl ether yielded yellow crystals of complex **3** (crystal yield: 46 mg, 60%). M.p. 170 °C. Anal. calcd (%) for $C_{180}H_{246}K_6N_{30}O_{71}P_2$: C 50.72, H 5.82, N 9.86; found: C 50.51, H 5.90, N 9.63.

[K(18-crown-6)]₆[(PO₄)₂(**L⁴**)₃] (**4**): Complex **4** was synthesized by a similar method to that used for **3**, from **L⁴** (36.6 mg, 0.5 mmol), K₃PO₄·10 H₂O (18.5 mg, 0.5 mmol), and 18-crown-6 (39.6 mg, 1.5 mmol), as yellow crystals (50 mg, 70%). M.p. 192 °C. Anal. calcd (%) for $C_{180}H_{240}K_6N_{30}O_{68}P_2$: C 51.37, H 5.75, N 9.98; found: C 51.03, H 5.87, N 9.66.

X-ray crystallography

Diffraction data were collected on a Bruker SMART APEX II diffractometer at 173 K with graphite-monochromated Mo-Kα radiation ($\lambda=0.71073$ Å) for complex **2** or Cu-K radiation ($\lambda=1.54178$ Å) for complex **3**. An empirical absorption correction using SADABS was applied for all data. The structures were solved by direct methods using the SHELXS program. All non-hydrogen atoms were refined anisotropically by full-matrix least-squares on F^2 by the use of the SHELXL program. Hydrogen atoms bonded to carbon and nitrogen were included in idealized geometric positions with thermal parameters equivalent to 1.2 times those of the atom to which they were attached. Hydrogen atoms on the water oxygen atoms for complex **3** were located from the difference Fourier map and then refined considering their chemical environments with restraints (O—H 0.85(2) Å), with U(H) fixed at 0.08 Å². Crystal data and refinement details of complexes **2** and **3** are given in the Supporting Information, Table S1. CCDC 902016 (**2**) and CCDC 902017 (**3**) contain the supplementary crystallographic data for this paper. These data can be obtained free of charge from The Cambridge Crystallographic Data Centre via www.ccdc.cam.ac.uk/data_request/cif.

Acknowledgements

[1] a) A. F. Williams, *Chem. Eur. J.* **1997**, *3*, 15; b) C. Kaes, A. Katz, M. W. Hosseini, *Chem. Rev.* **2000**, *100*, 3553; c) R. P. Cheng, S. H. Gellman, W. F. De-Grado, *Chem. Rev.* **2001**, *101*, 3219; d) T. Nakano, Y. Okamoto, *Chem. Rev.* **2001**, *101*, 4013; e) C. Schmuck, *Angew. Chem. Int. Ed.* **2003**, *42*, 2448; *Angew. Chem.* **2003**, *115*, 2552; f) D. Bradshaw, J. B. Claridge, E. J. Cussen, T. J. Prior, M. J. Rosseinsky, *Acc. Chem. Res.* **2005**, *38*, 273; g) E. Yashima, K. Maeda, H. Iida, Y. Furusho, K. Nagai, *Chem. Rev.* **2009**, *109*, 6102; h) Y. Ferrand, A. M. Kendhale, B. Kauffmann, A. Grelard, C. Marie, V. Blot, M. Pipelier, D. Dubreuil, I. Huc, *J. Am. Chem. Soc.* **2010**, *132*, 7858.

[2] a) S. Akine, T. Taniguchi, T. Nabeshima, *J. Am. Chem. Soc.* **2006**, *128*, 15765; b) A. V. Davis, D. Fiedler, M. Ziegler, A. Terpin, K. N. Raymond, *J. Am. Chem. Soc.* **2007**, *129*, 15354; c) C. Olivier, Z. Grote, E. Solari, R. Scopelliti, K. Severin, *Chem. Commun.* **2007**, 4000; d) B. El Aroussi, S. Zebret, C. Besnard, P. Perrottet, J. Hamacek, *J. Am. Chem. Soc.* **2011**, *133*, 10764.

[3] a) A. El-ghayoury, L. Douce, A. Skoulios, R. Ziessel, *Angew. Chem. Int. Ed.* **1998**, *37*, 2205; *Angew. Chem.* **1998**, *110*, 2327; b) R. Ziessel, L. Douce, A. El-ghayoury, A. Harriman, A. Skoulios, *Angew. Chem. Int. Ed.* **2000**, *39*, 1489; *Angew. Chem.* **2000**, *112*, 1549.

[4] a) D. H. Leung, R. G. Bergman, K. N. Raymond, *J. Am. Chem. Soc.* **2007**, *129*, 2746; b) C. J. Brown, R. G. Bergman, K. N. Raymond, *J. Am. Chem. Soc.* **2009**, *131*, 17530; c) C. J. Hastings, M. D. Pluth, R. G. Bergman, K. N. Raymond, *J. Am. Chem. Soc.* **2010**, *132*, 6938.

[5] a) A. Oleksi, A. G. Blanco, R. Boer, I. Usón, J. Aymamí, A. Rodger, M. J. Hannon, M. Coll, *Angew. Chem. Int. Ed.* **2006**, *45*, 1227; *Angew. Chem.* **2006**, *118*, 1249; b) C. Q. Zhao, J. Geng, L. Y. Feng, J. S. Ren, X. G. Qu, *Chem. Eur. J.* **2011**, *17*, 8209.

[6] a) C. Piguet, G. Bernardinelli, G. Hopfgartner, *Chem. Rev.* **1997**, *97*, 2005; b) M. Albrecht, *Chem. Rev.* **2001**, *101*, 3457; c) M. Borkovec, J. Hamacek, K. Zeckert, *Coord. Chem. Rev.* **2005**, *249*, 705.

[7] a) M. Albrecht, M. Schneider, H. Rottele, *Chem. Ber./Recueil.* **1997**, *130*, 615; b) M. Meyer, B. Kersting, R. E. Powers, K. N. Raymond, *Inorg. Chem.* **1997**, *36*, 5179; c) D. L. Caulder, K. N. Raymond, *J. Chem. Soc. Dalton Trans.* **1999**, 1185; d) F. Cui, S. Li, C. Jia, J. S. Mathieson, L. Cronin, X.-J. Yang, B. Wu, *Inorg. Chem.* **2012**, *51*, 179.

[8] a) M. Albrecht, S. Kotila, *Angew. Chem. Int. Ed. Engl.* **1995**, *34*, 2134; *Angew. Chem.* **1995**, *107*, 2285; b) M. Albrecht, *Chem. Soc. Rev.* **1998**, *27*, 281; c) M. Albrecht, I. Janser, H. Houjou, R. Fröhlich, *Chem. Eur. J.* **2004**, *10*, 2839; d) M. Albrecht, R. Fröhlich, *Bull. Chem. Soc. Jpn.* **2007**, *80*, 797.

[9] a) J. W. Steed, J. L. Atwood, *Supermolecular Chemistry (2nd ed.)*; John Wiley & Sons, Ltd, **2009**; b) J. L. Sessler, P. A. Gale, W.-S. Cho, *Anion Receptor Chemistry*; The Royal Society of Chemistry, Cambridge, **2006**; c) P. A. Gale, *Acc. Chem. Res.* **2006**, *39*, 465; d) P. A. Gale, *Chem. Soc. Rev.* **2010**, *39*, 3746; e) M. Wenzel, J. R. Hiscock, P. A. Gale, *Chem. Soc. Rev.* **2012**, *41*, 480.

[10] a) J.-M. Lehn, *Acc. Chem. Res.* **1978**, *11*, 49; b) K. Bowman-James, *Acc. Chem. Res.* **2005**, *38*, 671; c) B. P. Hay, T. K. Firman, B. A. Moyer, *J. Am. Chem. Soc.* **2005**, *127*, 1810; d) S. O. Kang, R. A. Begum, K. Bowman-James, *Angew. Chem. Int. Ed.* **2006**, *45*, 7882; *Angew. Chem.* **2006**, *118*, 8048; e) K. Bowman-James, A. Bianchi, E. García-España, Eds. *Anion Coordination Chemistry*, Wiley-VCH, Weinheim, **2011**.

[11] a) J. Sánchez-Quesada, C. Seel, P. Prados, J. de Mendoza, *J. Am. Chem. Soc.* **1996**, *118*, 277; b) J. Keegan, P. E. Kruger, M. Nieuwenhuyzen, J. O'Brien, N. Martin, *Chem. Commun.* **2001**, 2192; c) S. J. Coles, J. G. Frey, P. A. Gale, M. B. Hursthouse, M. E. Light, K. Navakhun, G. L. Thomas, *Chem. Commun.* **2003**, 568; d) Y. Haketa, H. Maeda, *Chem. Eur. J.* **2011**, *17*, 1485; e) R. Custelcean, P. V. Bonnesen, B. D. Roach, N. C. Duncan, *Chem. Commun.* **2012**, *48*, 7438.

[12] a) C. Jia, B. Wu, S. Li, X. Huang, X.-J. Yang, *Org. Lett.* **2010**, *12*, 5612; b) C. Jia, B. Wu, S. Li, X. Huang, Q. Zhao, Q.-S. Li, X.-J. Yang, *Angew. Chem. Int. Ed.* **2011**, *50*, 486; *Angew. Chem.* **2011**, *123*, 506; c) C. Jia, B. Wu, S. Li, Z. Yang, Q. Zhao, J. Liang, Q.-S. Li, X.-J. Yang, *Chem. Commun.* **2010**, *46*, 5376; d) S. Li, C. Jia, B. Wu, Q. Luo, X. Huang, Z. Yang, Q.-S. Li, X.-J. Yang, *Angew. Chem. Int. Ed.* **2011**, *50*, 5721; *Angew. Chem.* **2011**, *123*, 5839; e) B. Wu, F. Cui, Y. Lei, S. Li, N. D. S. Amadeu, C. Janiak, Y.-J. Lin, L.-H. Weng, Y.-Y. Wang, X.-J. Yang, *Angew. Chem. Int. Ed.* **2013**, *52*, 5096; *Angew. Chem.* **2013**, *125*, 5200; f) J. Zhao, D. Yang, Y. Zhao, X.-J. Yang, Y.-Y. Wang, B. Wu, *Angew. Chem. Int. Ed.* **2014**, *53*, 6632; *Angew. Chem.* **2014**, *126*, 6750.

[13] a) S. J. Brooks, P. A. Gale, M. E. Light, *Chem. Commun.* **2005**, 4696; b) S. J. Brooks, P. A. Gale, M. E. Light, *CrystEngComm* **2005**, *7*, 586; c) S. J. Moore, C. J. E. Haynes, J. Gonzalez, J. L. Sutton, S. J. Brooks, M. E. Light, J. Herniman, G. J. Langley, V. Soto-Cerrato, R. Perez-Tomas, I. Marques, P. J. Costa, V. Felix, P. A. Gale, *Chem. Sci.* **2013**, *4*, 103.

[14] a) Z. Hou, C. J. Sunderland, T. Nishio, K. N. Raymond, *J. Am. Chem. Soc.* **1996**, *118*, 5148; b) J. S. Fleming, K. L. V. Mann, C.-A. Carraz, E. Psillakis, J. C. Jeffery, J. A. McCleverty, M. D. Ward, *Angew. Chem. Int. Ed.* **1998**, *37*, 1279; *Angew. Chem.* **1998**, *110*, 1315.

[15] C. Janiak, *J. Chem. Soc. Dalton Trans.* **2000**, 3885.

[16] The selected models were built and optimized at the B3LYP/6–31G level, using the Gaussian 03 program suit (for more details and full citation, see the Supporting Information).

[17] Z. Zhang, D. Dolphin, *Inorg. Chem.* **2010**, *49*, 11550.